LETTERS

Angular Momenta of the Antarctic and the Arctic Oscillations

JIN-SONG VON STORCH

Max Planck Institute of Meteorology, Hamburg, Germany

17 September 1999 and 20 October 1999

ABSTRACT

The angular momentum anomalies associated with the Antarctic and Arctic Oscillations are examined in a coupled general circulation model. The size of the global-mean anomaly of the Ω angular momentum is unexpectedly larger than that of the relative angular momentum. The result is a simple consequence of mass conservation. Since the mass anomaly at high latitudes is equal and opposite to that at low latitudes, and since the high-latitude mass anomaly is relatively close to the rotation axis, the global-mean Ω angular momentum is significantly nonzero. Analysis of the meridional mass transport indicates that the Antarctic and Arctic Oscillations are persistent but damped modes.

1. Introduction

Thompson and Wallace (1998, 2000) found that the primary modes of the geopotential height field in each hemisphere are remarkably similar. Both modes, referred to as the Antarctic and the Arctic Oscillations (AAO and AO), are related to meridional dipoles in zonal-mean zonal wind field and to seesaws in atmospheric mass in the polar regions and the low-latitude zonal rings. While the similarity between the primary modes in the two hemispheres became more apparent in the recent studies of Thompson and Wallace, the AAO has been known for a long time. One of the early descriptions of the mode was given by Rogers and van Loon (1982).

This note studies the axial angular momentum of the AAO and the AO, a feature that has not been systematically considered so far. The 1000-yr integration with the coupled ECHAM1/LSG general circulation model (the Hamburg version of the European Centre Model coupled to the Large-Scale Geostrophic ocean model) is used for this purpose. The coupled model is developed at Max Planck Institute of Meteorology in Hamburg. A description of the coupled integration is given by von Storch et al. (1997). The early analysis using 500 yr of this integration (von Storch 1999) was concentrated on the first two EOFs of the global 200-hPa streamfunction field. The first one is related to zonal wind anomalies centered in the tropical upper troposphere and is highly correlated with the global relative angular momentum. The second mode is related to zonal wind anomalies similar to the AAO described by Thompson and Wallace (2000, hereafter TW00) and is highly correlated with the global Ω angular momentum. In the present note, the early analysis is extended to the third EOF of the global streamfunction field, which is related to zonal wind anomalies similar to those of the AO described by TW00.

In the following, the modes related to the second and third principal components (PC2 and PC3) of the 200-hPa stream function in the ECHAM1/LSG integration will be referred to as the (modeled) AAO and AO, respectively. The PCs are obtained from an EOF analysis of 1000-yr monthly anomalies. The corresponding EOF patterns are similar to those derived from 500 yr of data. The first three EOFs explain, respectively, 41%, 5.8%, and 3.4% of the variance of the 200-hPa streamfunction field. They are well separated and pass the rule of thumb of North et al. (1982). All results discussed below are obtained by regressing the considered variables, that is, 1000-yr monthly anomalies of zonal-mean zonal and meridional wind, $[u]$ and $[v]$, and zonally averaged surface pressure, $[p_s]$, upon the standardized PC2 and PC3. The results correspond to anomalies related to one standard deviation anomaly in PCs.

The key variable used is 200-hPa streamfunction, rather than geopotential height or pressure fields as in many previous studies. Concerning the AAO and the AO, the results of this paper are comparable to those derived from geopotential height or pressure fields. However, from the point of view of global angular momentum, both geopotential height and pressure are not optimal, since they cannot describe the mode related to global relative angular momentum (i.e., PC1 of 200-hPa

Corresponding author address: Dr. Jin-Song von Storch, Max-Planck-Institut für Meteorologie, Bundesstrasse 55, D-20146 Hamburg, Germany.
E-mail: jinsong@gkss.de

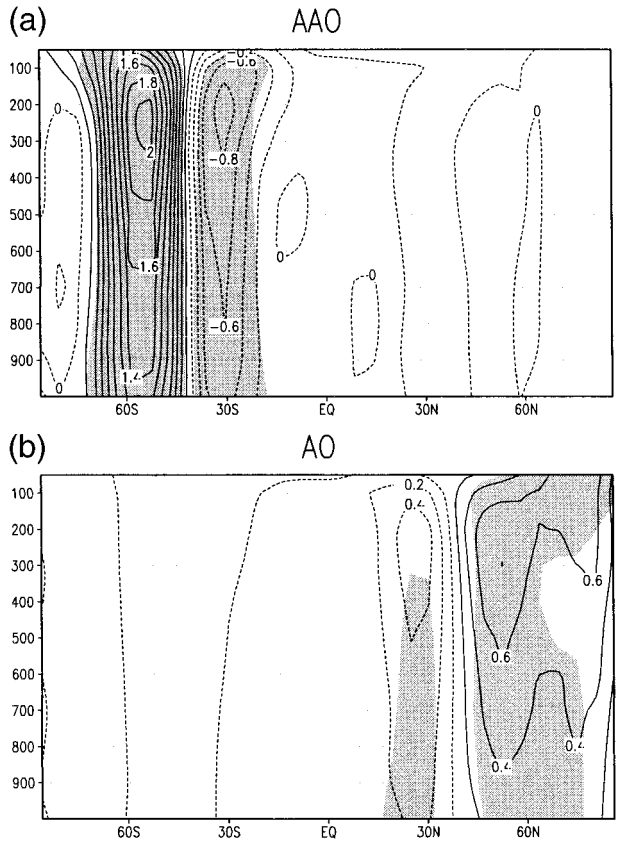

FIG. 1. Regression patterns of zonally averaged zonal wind [u] as a function of pressure (hPa) and latitude, related to (a) the AAO and (b) the AO. The shaded areas indicate the areas where the regression explains more than 10% of the total monthly variance. Contour intervals are 0.2 m s^{-1}. Solid (dashed) lines represent positive (negative) anomalies.

steamfunction). This mode is not associated with significant mass anomalies and does not show up in geopotential height or pressure fields. For the sake of completeness (in the context of angular momentum), this paper uses 200-hPa streamfunction to represent the AAO and the AO.

2. Results

a. Comparison with the observations

The regression patterns in [u] (Fig. 1) and the weighted surface pressure [p_s] cosφ (Fig. 2) suggest that, as in the observations, the AAO and the AO in the model are characterized by the meridional dipoles in the fields of zonal-mean zonal wind and mass. The nodes of the pressure dipoles are located around 50°, comparable to the position of the nodes of geopotential height dipole shown in TW00. As in the observations, the modeled AAO is stronger than the AO in the troposphere. Furthermore, the observed tendency for the high-latitude centers of [u] to be tilted poleward with height is also evident in the model. Thus, the important spatial features of the AAO and the AO are reproduced by the ECHAM1/LSG model. It is noted that the ECHAM1 model extends to 10 hPa and coarsely resolves the lower stratosphere.

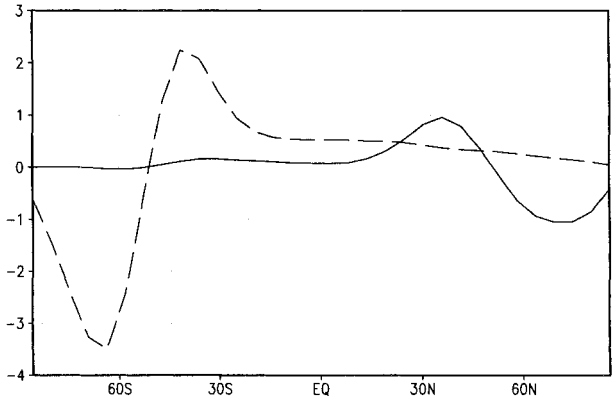

FIG. 2. Regression patterns of zonally averaged surface pressure [p_s] in hPa weighted by cosφ, related to the AAO (dashed line) and AO (solid line). The pressure anomaly at φ is proportional to the mass of the volume above the latitudinal belt at φ with unit width.

The main difference between the model result and the observations concerns the amplitudes of the modes. Both modes, in particularly the AO, are underestimated. For the high-latitude centers, the amplitude of zonal-mean zonal wind near 200 hPa is about 3 m s^{-1} in the Southern Hemisphere and about 1.5 m s^{-1} in the Northern Hemisphere in the observations (Fig.1 in TW00), whereas the corresponding values in the model are about 2 and 0.6 m s^{-1}, respectively. For the midlatitude centers, the underestimation is even stronger. Analyses of the variability in the ECHAM1/LSG integration suggest that the small amplitude of the modes reflects the general feature that the coupled model systematically underestimates variability on almost all timescales.

b. Angular momenta of the AAO and the AO

Using the hydrostatic approximation, the global axial relative and Ω angular momenta are given by

$$M_r = \int_V \rho r \cos\varphi u \, dV = \int_{-\pi/2}^{\pi/2} \mathbf{m}_r(\varphi), \tag{1}$$

$$M_\Omega = \int_V \rho \Omega r^2 \cos^2\varphi \, dV = \int_{-\pi/2}^{\pi/2} \mathbf{m}_\Omega(\varphi), \tag{2}$$

with

$$\mathbf{m}_r(\varphi) = \frac{2\pi r^2}{g} \int_0^{p_s} r \cos\varphi [u] \cos\varphi \, dp \, d\varphi, \tag{3}$$

$$\mathbf{m}_\Omega(\varphi) = \frac{2\pi r^2 \Omega}{g} (r \cos\varphi)^2 [p_s] \cos\varphi \, d\varphi, \tag{4}$$

where $\int_V dV$ is the integral over the volume of the model atmosphere, ρ density, r the radius of the earth, Ω the

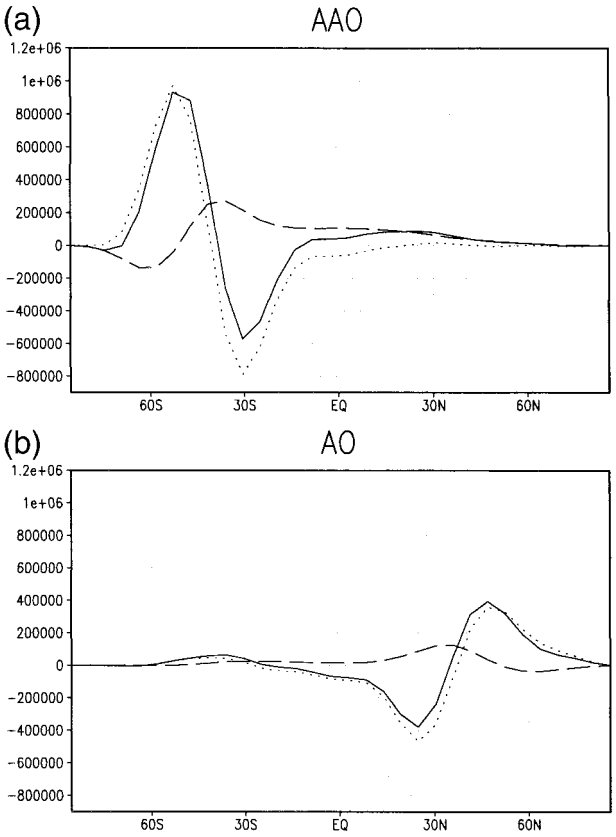

FIG. 3. Meridional profiles of $\mathbf{m}_r$ (dotted lines), $\mathbf{m}_\Omega$ (dashed lines), and $\mathbf{m}_r + \mathbf{m}_\Omega$ (solid lines), in Hadley seconds, for (a) the AAO and (b) the AO, where 1 Hadley $= 10^{18}$ kg m^2 s^{-2}.

angular velocity of the earth, φ latitude, g gravity, p pressure, and $\mathbf{m}_r$ and $\mathbf{m}_\Omega$ the relative and Ω angular momenta of the volume above a latitudinal belt with unit width.

Figure 3 shows $\mathbf{m}_r$ (dotted lines) and $\mathbf{m}_\Omega$ (dashed lines) calculated from Eqs. (3) and (4) using the regression patterns of $[u]$ and $[p_s]$. Dipole structures in $\mathbf{m}_r$ and $\mathbf{m}_\Omega$ are found for both the AAO and the AO. The amplitudes of the dipoles in $\mathbf{m}_r$ (dotted lines) are clearly larger than those in $\mathbf{m}_\Omega$ (dashed lines). Thus, from a local point of view, the relative angular momentum is more important than the Ω angular momentum.

One might expect from the difference in the amplitudes of the dipoles in $\mathbf{m}_r$ and $\mathbf{m}_\Omega$ that the global integral of $\mathbf{m}_r$ is also larger than the global integral of $\mathbf{m}_\Omega$. Table 1 shows that this is not the case. For the AO, the amplitude of the global Ω angular momentum is about a factor of 2.4 larger than that of the relative angular momentum. This ratio is larger and reaches 4.5 for the AAO.

The global angular momentum depends on the angular momenta of the low- and high-latitude centers in Fig. 3, which cancel each other. Table 1 suggests that the cancellation is much stronger for the relative angular momentum than for the Ω angular momentum. This feature is further described in Fig. 4, which shows the sums of, respectively, positive and negative $\mathbf{m}_r$ and $\mathbf{m}_\Omega$ anomalies. According to Fig. 3, the sum of positive $\mathbf{m}_r$ and that of negative $\mathbf{m}_\Omega$ represent essentially the angular momenta at the high latitudes (bars labeled with *H* in Fig. 4), and those of negative $\mathbf{m}_r$ and positive $\mathbf{m}_\Omega$ the angular momenta at the low latitudes (bars labeled with *L* in Fig. 4). For the comparison, the global angular momenta (black bars) are also given. The amplitudes of the relative angular momenta in the low-latitude centers are comparable to those in the high-latitude centers. It is not clear which center has larger angular momentum. For the AAO, the amplitude of the relative angular momentum in the high-latitude center is larger than that in the low-latitude center, but the opposite is true for the AO. The latter leads to the negative global value (see also Table 1). In contrast to that, the difference in the amplitudes of the Ω angular momenta of the low- and high-latitude centers is much more distinct. For both modes, the low-latitude center possesses significantly more Ω angular momentum than the high-latitude center. The global Ω angular momentum is determined to

TABLE 1. One std dev anomalies in relative (M_r) and Ω angular momentum (M_Ω) of the AAO and AO. Here M_r is calculated from the regression patterns of $[u]$, whereas M_Ω is calculated from the regression patterns of $[p_s]$. Both M_r and M_Ω are given in 10^6 Hadley seconds, where 1 Hadley $= 10^{18}$ kg m^2 s^{-2}.

	AAO	AO
M_r	0.38	−0.25
M_Ω	1.72	0.61
$\lvert M_\Omega/M_r \rvert$	4.5	2.4

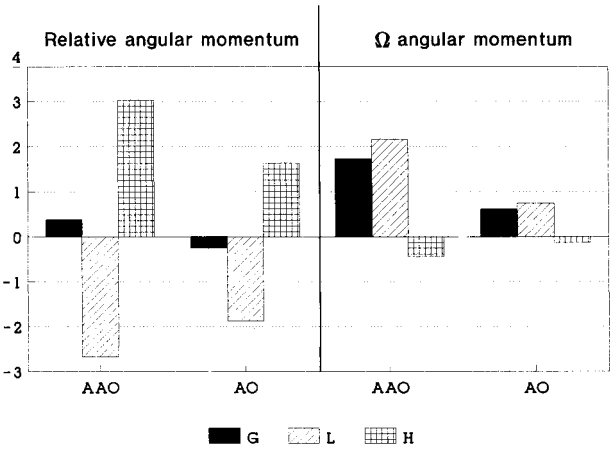

FIG. 4. The sums of positive and negative $\mathbf{m}_r$ (left) and the sums of positive and negative $\mathbf{m}_\Omega$ (right). The sums of the positive $\mathbf{m}_r$ and those of the negative $\mathbf{m}_\Omega$ represent essentially the relative and Ω angular momenta in the high-latitude centers and are marked by bars labeled with *H*. The sums of the negative $\mathbf{m}_r$ and those of the positive $\mathbf{m}_\Omega$ represent essentially the relative and Ω angular momenta in the low-latitude centers and are marked by bars labeled with *L*. The black bars indicate the global angular momenta. The unit is 10^6 Hadley second.

a large extent by the Ω angular momentum of the low-latitude center.

3. Discussion

a. *Why is the amplitude of the Ω angular momentum so large?*

The mass anomalies shown in Fig. 2 suggest that the mass is, to the first order, preserved for each mode (i.e., the possible imbalance induced by precipitation and evaporation is negligible). The integral of $[p_s]\cos\varphi$ over the low-latitude center, which extends with small amplitude across the equator into the other hemisphere, equals essentially the integral over the high-latitude center. On the other hand, the Ω angular momentum is obtained by weighting the mass anomalies with $(r\cos\varphi)^2$ [see Eq. (4)], which is the square of the distance from the considered position at the earth's surface to the earth's rotation axis. Since the high-latitude center is located much closer to the rotation axis than the low-latitude center, the condition of mass conservation must lead to the result that the low-latitude center has more Ω angular momentum than the high-latitude one, and the global Ω angular momentum is dominated by the Ω angular momentum of the low-latitude center.

Since the zonal-mean zonal wind is essentially in geostrophic balance with the meridional pressure gradient, the above-discussed constraint in the mass distribution can play an important role for the understanding of the global dynamics of the two modes.

b. *What maintains the anomalies in Ω angular momentum?*

Following Peixoto and Oort (1992, p. 248), the time rate of change of the global Ω angular momentum is essentially determined by the globally integrated meridional transport $\mathcal{C}$ (the vertical transport is zero in the ECHAM model). Here $\mathcal{C}$ is defined by

$$\mathcal{C} = \int_V (-2\Omega r\rho v\cos\varphi\,\sin\varphi)\,dV = \int_{-\pi/2}^{\pi/2} \mathbf{c}(\varphi), \quad (5)$$

with

$$\mathbf{c}(\varphi) = -\frac{4\pi\Omega r^3}{g}\int_0^{p_s} [v]\cos^2\varphi\,\sin\varphi\,dp\,d\varphi, \quad (6)$$

where the hydrostatic approximation is used. Further, $\mathbf{c}(\varphi)$ is the net meridional transport within the volume above a latitudinal belt with unit width. Note that $\mathbf{c}$ is proportional to $[v]$ in the Southern Hemisphere but to $-[v]$ in the Northern Hemisphere. Moving mass toward the equator, that is, away from the rotation axis, will result in a positive $\mathcal{C}$, which leads to an increase in Ω angular momentum.

Using Eq. (6), $\mathbf{c}(\varphi)$ is calculated from the regression patterns of $[v]$ [not shown; the regression upon PC2 is similar to Fig. 3d in von Storch (1999)]. These patterns suggest that, as in the observations, the mass dipole with positive anomalies at low latitudes and negative ones in the polar region is related to a meridional circulation with a convergent flow in the upper troposphere and a divergent flow near the surface. One can therefore further decompose the net transport $\mathbf{c}(\varphi)$ into $\mathbf{c}_u$ and $\mathbf{c}_l$, which represent, respectively, the contributions to $\mathbf{c}(\varphi)$ from the upper and lower branch of the meridional circulation.

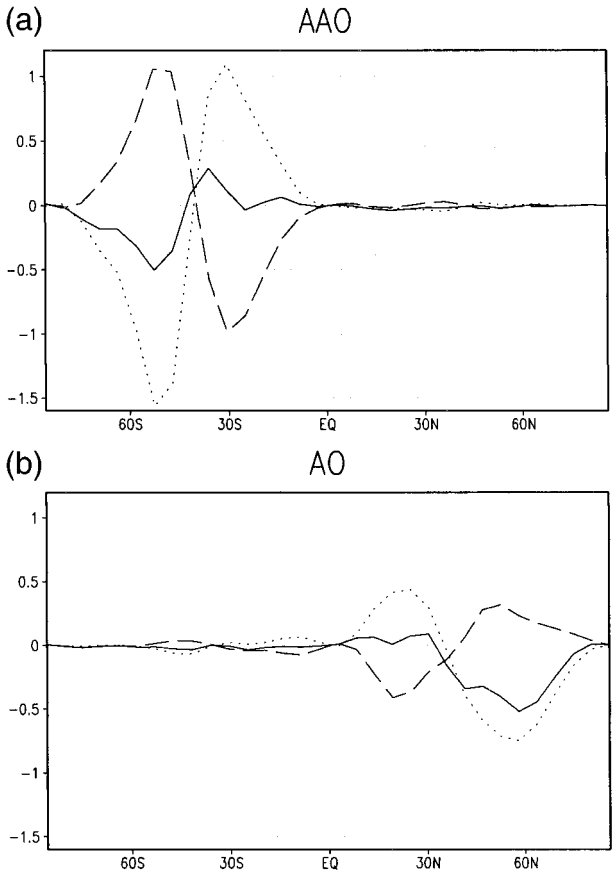

FIG. 5. Profiles of $\mathbf{c}_u(\varphi)$ (dashed lines), $\mathbf{c}_l(\varphi)$ (dotted lines), and $\mathbf{c}(\varphi)$ (solid lines), obtained from the regression patterns of zonal-mean meridional wind of (a) the AAO and (b) the AO. The transport of the upper branch of the meridional circulation, $\mathbf{c}_u$, is obtained by performing the vertical integration $\int dp$ in Eq. (6) from the top of the model atmosphere to 700 hPa, and the transport of the lower branch of the meridional circulation, $\mathbf{c}_l$, is obtained by performing the vertical integration from 700 hPa to the surface. The unit is Hadleys.

For both the AAO and the AO, a balance between $\mathbf{c}_u(\varphi)$ and $\mathbf{c}_l(\varphi)$ is found (Fig. 5). The nodes of the dipoles in $\mathbf{c}_u(\varphi)$ and $\mathbf{c}_l(\varphi)$ (dashed and dotted lines in Fig. 5) are located near 40°, where the center of positive anomalies of $\mathbf{m}_\Omega$ situates (dashed lines in Fig. 3). Recall the sign relation between $\mathbf{c}$ and $[v]$. The dipoles in $\mathbf{c}_u$ and $\mathbf{c}_l$ suggest a transport toward 40° by the upper branch and a transport away from 40° by the lower branch of the meridional circulation. To a large extent, the two transports balance each other. This balance acts

to maintain the $\mathbf{m}_\Omega$ anomalies at low latitudes centered at 40°. Since the low-latitude anomalies determine to a large extent the global Ω angular momentum (Fig. 4), the balance acts also to maintain the global Ω angular momentum. Both the AAO and the AO appear therefore as persistent modes.

The balance between $\mathbf{c}_u(\varphi)$ and $\mathbf{c}_l(\varphi)$ is, however, not perfect. For both modes, $\mathbf{c}_l$ (dotted line) dominates $\mathbf{c}_u$ (dashed line). This is particularly true at high latitudes, resulting in large negative anomalies of $\mathbf{c}(\varphi)$ (solid line) and a negative value of $C = \int \mathbf{c}(\varphi)\, d\varphi$. One has a net transport toward the poles and from that a removal of the existing M_Ω anomaly shown in Fig. 4. Thus, from the point of view of Ω angular momentum balance, the AAO and the AO are damped modes.

The meridional circulation is not only important for Ω angular momentum but also for relative zonal momentum. For both modes, anomalous equatorward (poleward) flow prevails in the upper troposphere at latitudes of westerly (easterly) wind anomalies. The Coriolis force acting on this flow produces a deceleration (an acceleration) of zonal momentum. In order to maintain zonal momentum anomalies, this momentum forcing must be balanced by an anomalous eddy convergence (divergence). Thus, as noted by Yoden et al. (1987), Karoly (1990), Kidson and Sinclair (1995), and Hartmann and Lo (1998), the meridional circulation, together with eddy momentum fluxes, maintains the zonal wind anomalies in the free atmosphere.

Thus, the meridional circulation affects not only the balance of mass, but also that of zonal momentum. In fact, the momentum balance is coupled to the mass balance through the meridional circulation (Peixoto and Oort 1992). A complete understanding of the AAO and AO requires the understanding of this coupling.

4. Conclusions

This paper studies the angular momenta of the AAO and the AO modeled by the ECHAM1/LSG model. Both modes, which are realistically simulated by the model, show similar angular momentum variations. The main result is that the global Ω angular momentum is about a factor of 2–4 larger than the global relative angular momentum. This result suggests that, even though the momentum balance is locally important, it is globally less significant than the mass balance.

The dominance of the Ω angular momentum is a consequence of mass conservation. If the mass deficit (excess) at the high latitudes results from the mass excess (deficit) at the low latitudes, the global Ω angular momentum must be significantly nonzero, since the high-latitude mass is located much closer to the rotation axis and has therefore less Ω angular momentum than the low-latitude mass. This global constraint can be crucial for the understanding of the global dynamics of the modes.

The modeled AAO and the AO are accompanied by a meridional circulation, as in the observations. This paper shows that the upper branch of this circulation tends to build up and the lower branch tends to remove the Ω angular momentum of the low-latitude mass and from that the global Ω angular momentum. To the first order, the two branches balance each other and act to maintain the Ω angular momentum anomalies, making the AAO and the AO be persistent. The balance, however, is not perfect. The net meridional mass transport is dominated by the transport of the lower branch, which acts to remove the global Ω angular momentum. In this sense, both the AAO and the AO are persistent but damped modes.

REFERENCES

Hartmann, D. L., and F. Lo, 1998: Wave-driven zonal flow vacillation in the Southern Hemisphere. *J. Atmos. Sci.,* **55,** 1303–1315.

Karoly, D. J., 1990: The role of transient eddies in low-frequency zonal variations of the Southern Hemisphere circulation. *Tellus,* **42A,** 41–50.

Kidson, J. W., and M. R. Sinclair, 1995: The influence of persistent anomalies on Southern Hemisphere storm tracks. *J. Climate,* **8,** 1938–1950.

North, G. R., T. L. Bell, R. F. Cahalan, and F. J. Moeng, 1982: Sampling errors in the estimation of empirical orthogonal functions. *Mon. Wea. Rev.,* **110,** 699–706.

Peixoto, J. P. and A. H. Oort, 1992: *Physics of Climate.* American Institute of Physics, 520 pp.

Rogers, J. C., and H. van Loon, 1982: Spatial variability of sea level pressure and 500 mb height anomalies over the Southern Hemisphere. *Mon. Wea. Rev.,* **110,** 1375–1392.

Thompson, D. W. J., and J. M. Wallace, 1998: The Arctic Oscillation signature in the wintertime geopotential height and temperature fields. *Geophys. Res. Lett.,* **25,** 1297–1300.

——, and ——, 2000: Annular modes in the extratropical circulation. Part I: Month-to-month variability. *J. Climate,* in press.

von Storch, J.-S., 1999: On the reddest atmospheric modes and the forcings of the spectra of these modes. *J. Atmos. Sci.,* **56,** 1614–1626.

——, V. Kharin, U. Cubasch, G. C. Hegerl, D. Schriever, H. von Storch, and E. Zorita, 1997: A description of a 1260-year control integration with the coupled ECHAM1/LSG general circulation model. *J. Climate,* **10,** 1526–1544.

Yoden, S., M. Shiotani, and I. Hirota, 1987: Multiple planetary flow regimes in the Southern Hemisphere. *J. Meteor. Soc. Japan,* **65,** 571–586.